AUT Journal of Mechanical Engineering

AUT J. Mech. Eng., 4(2) (2020) 151-168
DOI: 10.22060/ajme.2019.15561.5779

Robust Performance Analysis for a Cascade Nonlinear H∞ Control Algorithm in Quadrotor Position Tracking

F. Rekabi, F. A. Shirazi*, M. J. Sadigh

School of Mechanical Engineering, College of Engineering, University of Tehran, Tehran, Iran

ABSTRACT: This paper presents a new hierarchical robust algorithm to solve the position tracking problem, in presence of exogenous disturbances and modeling uncertainties, of a quadrotor helicopter. The suggested controller includes a nonlinear H_∞ algorithm to track the reference trajectory in the outer loop and a nonlinear H_∞ controller to stabilize the rotational movements in the inner loop. The resultant controller consists of three important parts to regulate tracking errors for translational and rotational motions, maintain robust performance confronting random disturbances and modeling uncertainties and reject the sustained disturbances from the system to vanish the steady-state errors. Analytical study on the stability of the cascade system is mentioned to verify the compatibility of two controllers considering coupling terms. Numerical performance analysis is accomplished using Monte-Carlo simulation. Statistical results obtained from 1000 simulations considering environmental disturbances and modeling uncertainties depict less than 5 cm for position tracking error and less than 2 degrees for attitude tracking error in steady state performance. The closed-loop performance of the controller is also compared with two previous algorithms by determining two numerical indexes for state tracking performance and control efforts, respectively. Simulation results of the suggested control algorithm depict a significant reduction in both indexes for a similar mission.

Review History:

Received: 31 Dec. 2018
Revised: 7 Apr. 2019
Accepted: 5 May. 2019
Available Online: 11 May. 2019

Keywords:

Position tracking
Nonlinear H_∞ control
Cascade control
Stability analysis

1- Introduction

Unmanned aerial vehicles, especially multirotors, have attracted a great interest in the automatic control area in last few decades due to their special advantages such as simple structure, vertical take-off and landing, rapid maneuvering and precise hovering. These vehicles have been used in tasks such as search and rescue, building exploration and security, and industrial inspections [1-3]. Although these vehicles have a high capability in aerial missions, their stabilization and control is challenging. The unstable and under-actuated nature of these systems makes the controller design procedure more complicated. Furthermore, quadrotors usually operate in presence of environmental disturbances such as wind gusts. Thus, quadrotors require not only a fast response hardware system but also a high performance control algorithm capable of confronting exogenous disturbing effects and uncertainties [4,5].

Control system design for quadrotors, has been highlighted in a number of papers and researchers have tried to satisfy the specifications by utilizing various techniques. In practice, especially in civil applications, low-cost equipment has been used for hardware, therefore it is crucial to compensate the consequent weaknesses by designing a simple structure algorithm with low computational burden for practical implementation. This controller has to consider the nonlinearities of the system and guarantees the stability of the closed-loop system [6-8]. Another work which presented a simple control algorithm to stabilize the quadrotor platform was presented in reference [9]. It resulted in a simple controller suitable for an embedded use when low computational resources are available. Some researchers have proposed a set of more complicated sensors to increase the reliability of the localization and obstacle avoidance systems. For instance, in reference [10] a Disturbance Observer Based (DOB) design was proposed that estimated the disturbance based on a dynamic model and a sensor suite including ultrasonic range finder and InfraRed (IR) sensors. In this work, the experimental results for robust controller based on this observer represented a good performance in harsh environments dangerous for the human to work. To handle the model uncertainty and external disturbances, different techniques have been used by researchers such as radial basis function neural networks adopted in the attitude control design and the backstepping technique [11-13]. A method for robustness against both environmental disturbance and parametric uncertainty was presented by Nicol et al. [14] using Cerebellar Model Articulation Controller (CMAC) nonlinear approximators for an experimental prototype quadrotor helicopter. The method updates adaptive parameters, the CMAC weights, as to achieve both adaptation and robustness to unknown payloads and disturbances. In a similar work, a robust-optimal control was proposed to compensate the parameter uncertainty effects and disturbances in reference [15]. In another work a robust-optimal framework was suggested using neural network to solve the position tracking

*Corresponding author's email: fshirazi@ut.ac.ir

problem for a quadrotor helicopter [16].

In a different way, some researchers used linear and nonlinear adaptive approaches to solve the attitude stabilization and path following problem for aerial robots [17-20]. Moreover, researchers have tried to apply nonlinear methods to conftont the complex dynamic behavior of these systems and improve the flying performance [21-23]. An underactuated NonLinear H_∞ (NLH_∞) controller based on the six degrees of freedom dynamic model was designed by Raffo et al. [24] to control the helicopter attitude and altitude in the inner-loop. The outer-loop control was performed using a Model-based Predictive Controller (MPC) to track the reference trajectory. The robust performance achieved by the proposed control strategy was checked by simulations in presence of aerodynamic disturbances, unmodelled dynamics, and parametric uncertainties but no theoretical proof of stability was presented for the cascade structure. Another work presented a method based on the block control technique combined with the super twisting control algorithm for trajectory tracking of a quadrotor helicopter in 2011. The performance and effectiveness of the proposed controller were tested in a simulation study taking into account external disturbances [25]. In another approach, a linear time-invariant controller consisting of a Proportional-Derivative (PD) controller and a robust compensator was used for robust attitude control of uncertain quadrotors. The PD controller was designed for the nominal linear system to achieve the desired tracking and the robust compensator was added to limit the influence of uncertainties. The simplicity of the final structure of control scheme made it applicable for practical cases with a simple hardware [11, 26-27]. Liu et al. [26] proposed a robust hierarchical controller including an attitude controller and a position controller. The position controller generated the desired reference of the pitch angle based on the tracking error of the travel angle, while the attitude controller achieved the reference tracking of the pitch and elevation angles. It was proven that the tracking errors of the three angles can converge to given neighborhoods ultimately. In another study by Zhao et al. [28], the control system was divided into two loops: the inner-loop for the attitude control and the outer-loop for the position. The sliding mode control technology was applied in the inner-loop to compensate the unmatched nonlinear disturbances, and the immersion and invariance approach was chosen for the outer-loop to address the parametric uncertainties. Another nonlinear adaptive-robust algorithm based on Invariance and Immersion algorithm and nonlinear H_∞ framework was presented in 2018 for robust trajectory tracking problem [19]. Despite the acceptable performance of this scheme in compensating random disturbances, this controller was not able to remove the errors caused by sustained disturbances. Also the nonlinear adaptive framework used for outer-loop was sensitive to parametric uncertainties, and the estimation and control performance was affected by this issue. Raffo et al. [29] in 2010 presented an integral predictive and nonlinear robust control strategy to solve the path following problem for a quadrotor helicopter. The proposed control structure was a hierarchical scheme consisting of a model predictive controller to track the reference trajectory together with a nonlinear H_∞ controller to stabilize the rotational movements capable of rejecting the effects of deterministic disturbances.

The previous algorithms suggested to solve the trajectory tracking problem have shown some drawbacks in practical cases. In linear approaches the final structure for the controller is simple enough for hardware implementation but this simplicity might lead to increased tracking errors. Applying nonlinear approaches can improve the tracking performance but in many cases the closed-loop response is sensitive to the model parameters and also the external disturbances. Utilizing approaches such as MPC or neural networks, conclude a complex framework which might not be appropriate for hardware implementation. The main contribution of this paper is to propose a new robust and nonlinear algorithm which consists of a unified stable control framework which has low computational burden and is simple enough for hardware implementation to solve the position tracking and attitude stabilization problem of a quadcopter. Considering previous studies on various types of algorithms and architectures utilized for this problem, it can be concluded that a cascade structure can be used as an appropriate architecture to regulate the position tracking error and stabilize the attitude dynamics, simultaneously. In this architecture, the outer-loop renders the position tracking problem, which uses the nonlinear H_∞ algorithm to estimate the position tracking error vector and compensate for it simultaneously. The inner-loop controller must be capable of stabilizing the attitude dynamics and rejecting both stochastic and deterministic disturbances. A suitable candidate to justify these requirements is the nonlinear H_∞ control method, which is combined with an integral action to regulate the steady state errors due to sustained disturbances.

After the presentation of analytical procedure for designing the suggested position tracking control framework, it is necessary to show the effectiveness and the acceptable performance of the proposed algorithm. To achieve this, a Monte-Carlo simulation process is proposed based on a detailed simulation environment to evaluate the robust performance of the closed-loop system, numerically. In this procedure, parametric uncertainties and two types of disturbances in 1000 simulations are considered. Accordingly, this procedure would be able to depict the average performance of the system as well as the bounds for the worst situation. Although there exist cascade controllers that use nonlinear and robust frameworks for position tracking, but they have not mentioned any proof for stability of the cascade system. In this paper, the proof of stability for cascade structure combining two nonlinear H_∞ is presented based on existing theories for stability analysis of the cascade controllers [30].

The remainder of the paper is organized as follows: in Section 2, an explanation of the dynamic model is given. In Section 3, the development of nonlinear H_∞ for the translational movements is presented. The nonlinear H_∞ controller for the rotational subsystem is presented in Section 4. The stability of the integrated inner and outer-loop controller is proven in Section 5. Simulation results are presented in Section 6. Finally, Section 7 concludes the paper.

2- Dynamic Modeling

In this paper, two reference frames are used to describe the position and attitude of the platform. The first one is the inertial frame defined as $\mathcal{I}$, and the second one is the body fixed frame described as $\mathcal{B}$. The center of $\mathcal{B}$ frame is attached to the center of mass of the platform and the position

vector of this point with respect to $\mathcal{I}$ frame is defined as $\xi^T(t)=[x(t)\quad y(t)\quad z(t)]\in\mathbb{R}^3$. The attitude vector with respect to $\mathcal{I}$ is defined as $\eta^T(t)=[\phi(t)\quad \theta(t)\quad \psi(t)]\in\mathbb{R}^3$. According to these definitions, the dynamic behavior of the quadrotor can be described by Eqs. (1) and (2) as follows:

$$m\ddot{\xi}+K_{\xi}\dot{\xi}+mG=F(t)+d_{\xi} \tag{1}$$

$$J(\eta)\ddot{\eta}+C_m(\eta,\dot{\eta})\dot{\eta}=\tilde{\tau}+d_{\eta} \tag{2}$$

where, m represents the mass of the platform, $J(\eta)$ denotes the inertial tensor defined in the inertial frame, K_{ξ} is the matrix of aerodynamic drag coefficients and belong to $\mathbb{R}^{3\times3}$. $C_m(\eta,\dot{\eta})$ denotes the matrix of coefficients related to attitude vector and rotational speed needed for computing the Coriolis effect and belongs to $\mathbb{R}^{3\times3}$. The force vector in the inertial frame is symbolized as $F(t)$ and the control torque described in inertial frame is denoted by $\tilde{\tau}$. Transformation matrix from body to the inertial frame is denoted by $R_t(\eta)$. The gravity acceleration vector in the inertial frame is represented by G. The effects of external disturbances and modelling uncertainties are defined by d_{ξ} and d_{η} for translational and rotational dynamics. It is also assumed that these terms belong to $\mathcal{L}_2(0,\infty)$. These equations are mainly taken from references [6,28] and the interested reader is referred to them. In this paper, the parameters of three matrices $J(\eta), K_{\xi}, K_r$ and the mass m, are assumed to be uncertain but the variation boundaries are known. In a quadrotor configuration, the actuator system includes four independent rotors. Accordingly, the system is naturally underactuated and to control the platform completely, two states are used as virtual control inputs to control the other states. It means that the cascaded structure is chosen for handling the rotational and translational dynamics simultaneously. In this case, roll and pitch angles are selected as virtual control signals to regulate the tracking error of the horizontal components of position vectors $x(t)$ and $y(t)$. Therefore, it is necessary to introduce a relative equation that can relate the desired value of attitude vector to the control force obtained from outer-loop controller utilized for regulating the position tracking error. The effects of actuator system can be described by Eq. (3) as follows:

$$\begin{cases} u_t=f_1+f_2+f_3+f_4 \\ \tau_x=l(-f_1-f_2+f_3+f_4) \\ \tau_y=l(-f_1+f_2+f_3-f_4) \\ \tau_z=c(-f_1+f_2-f_3+f_4) \end{cases} \tag{3}$$

where, f_i is the force generated by the i^{th} component of the actuator system. Two parameters l and c are the moment arm and yaw moment factor which convert the force to moment vector. Therefore, $F(t)$ in Eq. (1) is defined as follows.

$$F(t)=R_t(\eta)\begin{bmatrix}0\\0\\u_t\end{bmatrix} \tag{4}$$

It can be assumed that $F(t)$ includes three independent components described as $F^T(t)=[f_x(t)\quad f_y(t)\quad f_z(t)]$. Therefore, the relation between these components and euler angles can be written as follows.

$$\begin{cases} f_x(t)=u_t(\cos\phi\sin\theta\cos\psi+\sin\phi\sin\psi) \\ f_y(t)=u_t(\cos\phi\sin\theta\sin\psi-\sin\phi\cos\psi) \\ f_z(t)=u_t\cos\phi\cos\theta \end{cases} \tag{5}$$

According to Eq. (5), if three components of the force vector are estimated from position controller loop, the desired values of roll and pitch angles can be determined accordingly. The explicit relation used to determine the desired value of roll and pitch angles is introduced in the following equation where, $S\psi=\sin\psi$ and $C\psi=\cos\psi$.

$$\begin{cases} u_t &= \sqrt{f_x(t)^2+f_y(t)^2+f_z(t)^2} \\ \sin(\phi_d) &= \dfrac{f_x(t)S\psi_d-f_y(t)C\psi_d}{u_t} \\ \tan(\theta_d) &= \dfrac{f_x(t)C\psi_d+f_y(t)S\psi_d}{f_z(t)} \end{cases} \tag{6}$$

The controller design procedure for the system is divided into three steps according to a cascade architecture as follows:

1. Design the outer-loop controller for the path following problem assuming three independent control force components, and determine the desired value of the attitude vector.
2. Design the inner-loop controller to stabilize the attitude subsystem and track the desired value coming from the outer loop.
3. Prove the stability and boundedness of the cascade system considering the coupling terms between the inner and outer loops.

The remaining parts of this paper are organized to illustrate the above steps in more details.

3- Outer-Loop Contoller

In this section, the design procedure for the outer-loop controller is presented. Nonlinear H_{∞} scheme is suggested as an appropriate framework to design a robust controller able to compensate both external disturbances and modeling uncertainties. Hence, it is necessary to modify the translational motion dynamic equation into a proper form consistent with NL H_{∞} framework. The error signal presenting the difference between system states and desired values is defined as

$$e_\xi = \begin{bmatrix} \xi - \xi_d \\ \dot{\xi} - \dot{\xi}_d \\ \int \left(\xi - \xi_d \right) \end{bmatrix} \in \mathbb{R}^{9\times 1} \tag{7}$$

where, $\xi_d \in \mathbb{R}^3$ represents the desired path in three-dimensional space and $\dot{\xi}_d \in \mathbb{R}^3$ is the corresponding velocity vector. According to Eq. (1), the following expression is suggested as the control effort applied to the system.

$$\begin{aligned} f_c = {} & m\ddot{\xi} + K_\xi \dot{\xi} + mG \\ & - T_{1\xi}^{-1} \left(m T_\xi \dot{e}_\xi + K_\xi T_\xi e_\xi \right) + T_{1\xi}^{-1} q \end{aligned} \tag{8}$$

This control scheme is composed of three segments. The first part corresponds to the left side of Eq. (1). The second part consists of two terms for regulating the error signal, and the third part is considered for disturbance attenuation and robustness against parameter uncertainty. In Eq. (8), T_ξ is defined as $T_\xi = [T_{1\xi} \quad T_{2\xi} \quad T_{3\xi}] \in \mathbb{R}^{3\times 9}$ composed of three 3×3 matrices. Using Eq. (8) as control force, and substituting it into Eq. (1), the position tracking error dynamics will be obtained from the following equation.

$$m T_\xi \ddot{e}_\xi + K_\xi T_\xi \dot{e}_\xi = q + T_{1\xi} d_\xi \tag{9}$$

A more explicit form of Eq. (9) can be written as follows:

$$\dot{e}_\xi = T_{0\xi}^{-1} \begin{bmatrix} -\frac{K_\xi}{m} & 0 & 0 \\ T_{1\xi}^{-1} & I - T_{1\xi}^{-1} T_{2\xi} & -I - T_{1\xi}^{-1} \left(T_{3\xi} - T_{2\xi} \right) \\ 0 & I & -I \end{bmatrix} T_{0\xi} e_\xi \tag{10}$$

$$\text{where} T_{0\xi} = \begin{bmatrix} T_{1\xi} & T_{2\xi} & T_{3\xi} \\ 0 & I & I \\ 0 & 0 & I \end{bmatrix} \in \mathbb{R}^{9\times 9}, \text{ and } w = T_{1\xi} d_\xi \in \mathbb{R}^3.$$

Therefore, the error dynamics in Eq. (3) obtains a general form suitable for NLH_∞ design [31] as follows.

$$\dot{e}_\xi = f_\xi \left(e_\xi \right) + g_\xi \left(e_\xi \right) q + k_\xi \left(e_\xi \right) w \tag{11}$$

Comparing Eqs. (10) and (11), the system matrices will be defined as follows in Eqs. (12) and (13).

$$f_\xi \left(e_\xi \right) = T_{0\xi}^{-1} \begin{bmatrix} -\frac{K_\xi}{m} & 0 & 0 \\ T_{1\xi}^{-1} & I - T_{1\xi}^{-1} T_{2\xi} & -I - T_{1\xi}^{-1} \left(T_{3\xi} - T_{2\xi} \right) \\ 0 & I & -I \end{bmatrix} T_{0\xi} e_\xi \tag{12}$$

$$g_\xi \left(e_\xi \right) = k_\xi \left(e_\xi \right) = T_{0\xi}^{-1} \begin{bmatrix} \frac{1}{m} I \\ 0 \\ 0 \end{bmatrix} \tag{13}$$

If the performance index is defined as $\zeta_\xi = W_\xi \begin{bmatrix} e_\xi \\ q \end{bmatrix}$,

where $W_\xi \in \mathbb{R}^{1\times 12}$ is a weight matrix, then the NLH_∞ can be stated as follows:

"Find the smallest value $\gamma^* \geq 0$ such that for any $\gamma \geq \gamma^*$ there exists a state feedback $q = q\left(e_\xi, t \right)$, such that the l_2 gain from w to ζ_ξ is less than or equal to γ, that is:"

$$\int_0^T \| \zeta_\xi \|_2^2 \, dt \leq \gamma^2 \int_0^T \| w \|_2^2 \, dt \tag{14}$$

The internal term of integral expression of the performance index can be rewritten as Eq. (15):

$$\| \zeta_\xi \|_2^2 = \begin{bmatrix} e_\xi^T & q^T \end{bmatrix} W_\xi^T W_\xi \begin{bmatrix} e_\xi \\ q \end{bmatrix} \tag{15}$$

Since $W_\xi^T W_\xi$ is symmetric and positive definite, it can be decomposed into 3 basic weight matrices as follows:

$$W_\xi^T W_\xi = \begin{bmatrix} Q_\xi & S_\xi \\ S_\xi^T & R_\xi \end{bmatrix} \tag{16}$$

where, Q_ξ and R_ξ are two symmetric and positive definite matrices and $Q_\xi - S_\xi R_\xi^{-1} S_\xi^T \geq 0$. To solve this problem, it is necessary to define a Lyapunov function $V_\xi \left(e_\xi \right)$ which satisfies the Hamilton Jacobi Bellman (HJB) equation stated in the following [31].

$$\frac{\partial V_\xi}{\partial t}+\frac{\partial^T V_\xi}{\partial e_\xi} f_\xi\left(e_\xi,t\right)$$

$$+\frac{1}{2}\frac{\partial^T V_\xi}{\partial e_\xi}\left(\frac{1}{\gamma^2}k_\xi\left(e_\xi,t\right)k_\xi^T\left(e_\xi,t\right)-g_\xi\left(e_\xi,t\right)R_\xi^{-1}g_\xi\left(e_\xi,t\right)\right)\frac{\partial V_\xi}{\partial e_\xi} \quad (17)$$

$$-\frac{\partial^T V_\xi}{\partial e_\xi} g_\xi\left(e_\xi,t\right)R_\xi^{-1}S_\xi^T e_\xi+\frac{1}{2}e_\xi^T\left(Q_\xi-S_\xi R_\xi^{-1}S_\xi^T\right)e_\xi=0$$

Theorem 1:

Suppose a Lyapunov function $V_\xi\left(e_\xi,t\right)=\frac{1}{2}e_\xi^T T_{0\xi}^T \nu_\xi\left(e_\xi\right)T_{0\xi}e_\xi$

where, $\nu\left(e_\xi\right)$ is a symmetric and positive definite matrix with the following structure:

$$\left(e_\xi\right)=\begin{bmatrix} mI & 0 & 0 \\ 0 & Y_\xi & X_\xi-Y_\xi \\ 0 & X_\xi-Y_\xi & Z_\xi+Y_\xi \end{bmatrix} \quad (18)$$

where, $X_\xi,Y_\xi,Z_\xi\in\mathbb{R}^{3\times3}$ are three symmetric and positive definite matrices and $Z_\xi-X_\xi Y_\xi^{-1}X_\xi+2X_\xi\geq0$. Using the proposed Lyapunov function, the HJB equation in Eq. (17) is constituted if the following holds.

$$-2T_\xi^T K_\xi T_\xi+\begin{bmatrix} 0 & Y_\xi & X_\xi \\ Y_\xi & 2X_\xi & Z_\xi+2X_\xi \\ X_\xi & Z_\xi+2X_\xi & 0 \end{bmatrix}+Q_\xi \quad (19)$$

$$+\frac{1}{\gamma^2}T_\xi^T T_\xi-(S_\xi^T+T_\xi)^T R_\xi^{-1}\left(S_\xi^T+T_\xi\right)=0$$

Proof:

To demonstrate the validity of Theorem 1, it is necessary to expand the HJB equation. From Eqs. (11) and (12), the Eqs. (20) to (24) can be concluded as follows.

$$\frac{\partial V_\xi}{\partial e_\xi}=T_{0\xi}^T\begin{bmatrix} mI & 0 & 0 \\ 0 & Y_\xi & X_\xi-Y_\xi \\ 0 & X_\xi-Y_\xi & Z_\xi+Y_\xi \end{bmatrix}T_{0\xi}e_\xi \quad (20)$$

Hence, the second term of the HJB is derived to be as Eq. (21):

$$\frac{\partial^T V_\xi}{\partial e_\xi} f_\xi\left(e_\xi,t\right)=$$

$$e_\xi^T T_{0\xi}^T\begin{bmatrix} -K_\xi & 0 \\ T_{1\xi}^{-1}Y_\xi & X_\xi-T_{1\xi}^{-1}Y_\xi T_{2\xi} \\ T_{1\xi}^{-1}\left(X_\xi-Y_\xi\right) & X_\xi+Z_\xi-T_{1\xi}^{-1}\left(X_\xi-Y_\xi\right)T_{2\xi} \end{bmatrix} \quad (21)$$

$$\begin{bmatrix} 0 \\ -\left(X_\xi+T_{1\xi}^{-1}Y_\xi\left(T_{3\xi}-T_{2\xi}\right)\right) \\ -\left(X_\xi+Z_\xi+T_{1\xi}^{-1}\left(X_\xi-Y_\xi\right)\left(T_{3\xi}-T_{2\xi}\right)\right) \end{bmatrix}T_{0\xi}e_\xi$$

After multiplying the inner matrices and simplifying the results, Eq. (21) can be written as follows:

$$\frac{\partial^T V_\xi}{\partial e_\xi} f_\xi\left(e_\xi,t\right)=$$

$$e_\xi^T\begin{bmatrix} -T_{1\xi}^T K_\xi T_{1\xi} & -T_{1\xi}^T K_\xi T_{2\xi} \\ -T_{2\xi}^T K_\xi T_{1\xi}+Y_\xi & -T_{2\xi}^T K_\xi T_{2\xi}+X_\xi \\ -T_{3\xi}^T K_\xi T_{1\xi}+X_\xi & -T_{3\xi}^T K_\xi T_{2\xi}+2X_\xi+Z_\xi \end{bmatrix} \quad (22)$$

$$\begin{bmatrix} -T_{1\xi}^T K_\xi T_{3\xi} \\ -T_{2\xi}^T K_\xi T_{3\xi} \\ -T_{3\xi}^T K_\xi T_{3\xi} \end{bmatrix}e_\xi$$

Eq. (22) can be divided into two parts; the first one is composed of only X_ξ,Y_ξ,Z_ξ and the second one is a quadratic term based on matrix T_ξ. Eq. (23) shows this expression as follows.

$$\frac{\partial^T V_\xi}{\partial e_\xi} f_\xi\left(e_\xi,t\right)=e_\xi^T\left(\begin{bmatrix} 0 & 0 & 0 \\ Y_\xi & X_\xi & 0 \\ X_\xi & 2X_\xi+Z_\xi & 0 \end{bmatrix}-T_\xi^T K_\xi T_\xi\right)e_\xi \quad (23)$$

Since the term is a scalar and it equals to its transpose, Eq. (23) can be written as follows.

$$\frac{\partial^T V_\xi}{\partial e_\xi} f_\xi\left(e_\xi,t\right)=$$

$$e_\xi^T\left(-T_\xi^T K_\xi T_\xi+\frac{1}{2}\begin{bmatrix} 0 & Y_\xi & X_\xi \\ Y_\xi & 2X_\xi & 2X_\xi+Z_\xi \\ X_\xi & 2X_\xi+Z_\xi & 0 \end{bmatrix}\right)e_\xi \quad (24)$$

The next two terms of HJB equation are evolved in Eq. (25).

$$\frac{1}{2}\frac{\partial^T V_\xi}{\partial e_\xi}\left(\frac{1}{\gamma^2}k_\xi k_\xi^T - g_\xi R_\xi^{-1} g_\xi^T\right)\frac{\partial V_\xi}{\partial e_\xi} = \frac{1}{2}e_\xi^T T_\xi^T\left(\frac{1}{\gamma^2}\left(I-\gamma^2 R_\xi^{-1}\right)\right)T_\xi e_\xi \tag{25}$$

$$\frac{\partial^T V_\xi}{\partial e_\xi} g_\xi R_\xi^{-1} S_\xi^T e_\xi = e_\xi^T T_\xi^T R_\xi^{-1} S_\xi^T e_\xi$$

After substituting Eqs. (24) and (25) into HJB equation and simplifying it, the following expression will be obtained.

$$e_\xi^T\left(-2T_\xi^T K_\xi T_\xi + \begin{bmatrix} 0 & Y_\xi & X_\xi \\ Y_\xi & 2X_\xi & Z_\xi+2X_\xi \\ X_\xi & Z_\xi+2X_\xi & 0 \end{bmatrix} + Q_\xi + \frac{1}{\gamma^2}T_\xi^T T_\xi - \left(S_\xi^T + T_\xi\right)^T R_\xi^{-1}\left(S_\xi^T + T_\xi\right)\right) + e_\xi = 0 \tag{26}$$

Therefore, if Eq. (19) is justified, the HJB equation will be satisfied using the proposed Lyapunov function. Accordingly, the optimal state feedback control law can be derived from Eq. (27) as follows:

$$q^* = -R_\xi^{-1}\left(S_\xi^T e_\xi + g_\xi^T\frac{\partial V_\xi}{\partial e_\xi}\right) \tag{27}$$

the other hand, three matrices $T_{1\xi}, T_{2\xi}, T_{3\xi}$ used in Eq. (8) must be calculated to be used in the control law. To do this, it is necessary to solve Eq. (19) based on these matrices. The following shows an expanded expression of Eq. (19).

$$\begin{bmatrix} T_{1\xi}^T\Gamma_\xi T_{1\xi} & T_{1\xi}^T\Gamma_\xi T_{2\xi} & T_{1\xi}^T\Gamma_\xi T_{3\xi} \\ T_{2\xi}^T\Gamma_\xi T_{1\xi} & T_{2\xi}^T\Gamma_\xi T_{2\xi} & T_{2\xi}^T\Gamma_\xi T_{3\xi} \\ T_{3\xi}^T\Gamma_\xi T_{1\xi} & T_{3\xi}^T\Gamma_\xi T_{2\xi} & T_{3\xi}^T\Gamma_\xi T_{3\xi} \end{bmatrix} + \begin{bmatrix} Q_{1\xi} & Q_{12\xi} & Q_{13\xi} \\ Q_{12\xi} & Q_{2\xi} & Q_{23\xi} \\ Q_{13\xi} & Q_{22\xi} & Q_{13\xi} \end{bmatrix} - \begin{bmatrix} S_{1\xi}R_\xi^{-1}S_{1\xi}^T & S_{1\xi}R_\xi^{-1}S_{2\xi}^T & S_{1\xi}R_\xi^{-1}S_{3\xi}^T \\ S_{2\xi}R_\xi^{-1}S_{1\xi}^T & S_{2\xi}R_\xi^{-1}S_{2\xi}^T & S_{2\xi}R_\xi^{-1}S_{3\xi}^T \\ S_{3\xi}R_\xi^{-1}S_{1\xi}^T & S_{3\xi}R_\xi^{-1}S_{2\xi}^T & S_{3\xi}R_\xi^{-1}S_{3\xi}^T \end{bmatrix}$$
$$- \begin{bmatrix} S_{1\xi}R_\xi^{-1}T_{1\xi} & S_{1\xi}R_\xi^{-1}T_{2\xi} & S_{1\xi}R_\xi^{-1}T_{3\xi} \\ S_{2\xi}R_\xi^{-1}T_{1\xi} & S_{2\xi}R_\xi^{-1}T_{2\xi} & S_{2\xi}R_\xi^{-1}T_{3\xi} \\ S_{3\xi}R_\xi^{-1}T_{1\xi} & S_{3\xi}R_\xi^{-1}T_{2\xi} & S_{3\xi}R_\xi^{-1}T_{3\xi} \end{bmatrix} - \begin{bmatrix} T_{1\xi}^T R_\xi^{-1}S_{1\xi}^T & T_{1\xi}^T R_\xi^{-1}S_{2\xi}^T & T_{1\xi}^T R_\xi^{-1}S_{3\xi}^T \\ T_{2\xi}^T R_\xi^{-1}S_{1\xi}^T & T_{2\xi}^T R_\xi^{-1}S_{2\xi}^T & T_{2\xi}^T R_\xi^{-1}S_{3\xi}^T \\ T_{3\xi}^T R_\xi^{-1}S_{1\xi}^T & T_{3\xi}^T R_\xi^{-1}S_{2\xi}^T & T_{3\xi}^T R_\xi^{-1}S_{3\xi}^T \end{bmatrix}$$
$$+ \begin{bmatrix} 0 & Y_\xi & X_\xi \\ Y_\xi & 2X_\xi & 2X_\xi+Z_\xi \\ X_\xi & 2X_\xi+Z_\xi & 0 \end{bmatrix} = 0 \tag{28}$$

where, $\tilde{A}_\xi = -2K_\xi + \frac{1}{\gamma^2}I - R_\xi^{-1}$. According to Eq. (28), $T_{1\xi}, T_{2\xi}, T_{3\xi}$ can be calculated by solving at least 4 Riccati equations as presented in the following procedure:

1. Calculate $T_{1\xi}$ and $T_{3\xi}$ based on Eq. (29):

$$T_{1\xi}^T\Gamma_\xi T_{1\xi} + Q_{1\xi} - S_{1\xi}R_\xi^{-1}S_{1\xi}^T - S_{1\xi}R_\xi^{-1}T_{1\xi} - T_{1\xi}^T R_\xi^{-1}S_{1\xi}^T = 0$$
$$T_{3\xi}^T\Gamma_\xi T_{3\xi} + Q_{3\xi} - S_{3\xi}R_\xi^{-1}S_{3\xi}^T - S_{3\xi}R_\xi^{-1}T_{3\xi} - T_{3\xi}^T R_\xi^{-1}S_{3\xi}^T = 0 \tag{29}$$

2. Calculate X_ξ using Eq. (30):

$$X_\xi = -T_{1\xi}^T\Gamma_\xi T_{3\xi} - Q_{13\xi} + S_{1\xi}R_\xi^{-1}S_{3\xi}^T + S_{1\xi}R_\xi^{-1}T_{3\xi} + T_{1\xi}^T R_\xi^{-1}S_{3\xi}^T \tag{30}$$

3. Calculate $T_{2\xi}$ using Eq. (31):

$$T_{2\xi}^T\Gamma_\xi T_{2\xi} + Q_{2\xi} + 2X_\xi - S_{2\xi}R_\xi^{-1}S_{2\xi}^T - S_{2\xi}R_\xi^{-1}T_{2\xi} - T_{2\xi}^T R_\xi^{-1}S_{2\xi}^T = 0 \tag{31}$$

Using matrices $T_{1\xi}, T_{2\xi}$ and $T_{3\xi}$ derived from above procedure and Eq. (27), the control law can be obtained as Eq. (32).

$$q^* = -R_\xi^{-1}\left(S_\xi^T + T_\xi\right)e_\xi \tag{32}$$

Hence, the optimal control force f_c^* which guarantees the position tracking performance in the presence of external disturbances and parameter uncertainties can be written as

$$f_c^* = m\ddot{\xi}_d + K_\xi \dot{\xi} + mG - m\begin{bmatrix} T_{1\xi}^{-1}T_{2\xi} + \frac{1}{m}T_{1\xi}^{-1}K_\xi T_{1\xi} + T_{1\xi}^{-1}R_\xi^{-1}\left(S_{1\xi}^T + T_{1\xi}\right) \\ T_{1\xi}^{-1}T_{3\xi} + \frac{1}{m}T_{1\xi}^{-1}K_\xi T_{2\xi} + T_{1\xi}^{-1}R_\xi^{-1}\left(S_{2\xi}^T + T_{2\xi}\right) \\ \frac{1}{m}T_{1\xi}^{-1}K_\xi T_{3\xi} + T_{1\xi}^{-1}R_\xi^{-1}\left(S_{3\xi}^T + T_{3\xi}\right) \end{bmatrix}^T e_\xi \quad (33)$$

Therefore, the control law can be stated in a Project Initiation Documentation (PID[1]) framework as Eq. (34):

$$f_c^* = m\ddot{\xi}_d + K_\xi \dot{\xi} + mG - m\left(K_{P\xi}\left(\xi - \xi_d\right) + K_{I\xi}\int\left(\xi - \xi_d\right)dt + K_{D\xi}\left(\dot{\xi} - \dot{\xi}_d\right)\right) \quad (34)$$

where, $K_{P\xi}$, $K_{I\xi}$ and $K_{D\xi}$ can be evaluated by comparing Eqs. (34) and (33) as mentioned in Eq. (35).

$$\begin{cases} K_{P\xi} = T_{1\xi}^{-1}T_{3\xi} + \frac{1}{m}T_{1\xi}^{-1}K_\xi T_{2\xi} + T_{1\xi}^{-1}R_\xi^{-1}\left(S_{2\xi}^T + T_{2\xi}\right) \\ K_{I\xi} = \frac{1}{m}T_{1\xi}^{-1}K_\xi T_{3\xi} + T_{1\xi}^{-1}R_\xi^{-1}\left(S_{3\xi}^T + T_{3\xi}\right) \\ K_{D\xi} = T_{1\xi}^{-1}T_{2\xi} + \frac{1}{m}T_{1\xi}^{-1}K_\xi T_{1\xi} + T_{1\xi}^{-1}R_\xi^{-1}\left(S_{1\xi}^T + T_{1\xi}\right) \end{cases} \quad (35)$$

For more simplicity the following assumptions were made for weight matrices:

$$\begin{cases} Q_{1\xi} = \omega_{1\xi}^2 I; Q_{2\xi} = \omega_{2\xi}^2 I; Q_{3\xi} = \omega_{3\xi}^2 I \\ Q_{12\xi} = Q_{13\xi} = Q_{23\xi} = 0 \\ S_{1\xi} = S_{2\xi} = S_{3\xi} = 0 \\ R_\xi = r_\xi^2 I \end{cases}$$

Therefore, the expression for controller gains reduce to the following form:

$$\begin{cases} K_{P\xi} = \left(\frac{\sqrt{\omega_{2\xi}^2 + 2\omega_{1\xi}\omega_{3\xi}}}{mr_\xi^2\omega_{1\xi}} + \frac{\omega_{3\xi}}{\omega 1\xi}\right)I + \frac{\sqrt{\omega_{2\xi}^2 + 2\omega_{1\xi}\omega_{3\xi}}}{m\omega_{1\xi}}K_\xi \\ K_{I\xi} = \frac{\omega_{3\xi}}{mr_\xi^2\omega_{1\xi}}I + \frac{\omega_{3\xi}}{m\omega_{1\xi}}K_\xi \\ K_{D\xi} = \left(\frac{1}{mr_\xi^2} + \frac{\sqrt{\omega_{2\xi}^2 + 2\omega_{1\xi}\omega_{3\xi}}}{\omega_{1\xi}}\right)I + \frac{1}{m}K_\xi \end{cases} \quad (36)$$

where, the parameters $\omega_{1\xi}, \omega_\xi, \omega_{3\xi}$ and r_ξ, are scalar parameters and can be used for controller tunning. It must be mentioned that the final expression for the control law depends only on general parameters of the system, e.g., mass and speed. In addition, it does not depend on γ, and has an algebraic form for this special case.

4- Inner-Loop Controller

The design procedure for the inner-loop controller based on nonlinear H_∞ is presented in this section. According to previous sections the rotational dynamic motion is affected by two sources of torque. Therefore, the net torque acting on the system can be introduced by the Eq. (37)

$$\tau_\eta = \tau_\eta + d_\tau \quad (37)$$

where, $\tilde{\tau}_\eta$ is the control torque acting on the system and d_η is the disturbance torque composed of both random and stationary components. State equation for determining the control law is defined as Eq. (38).

$$e_\eta = \begin{bmatrix} \dot{\eta} - \dot{\eta}_d \\ \eta - \eta_d \\ \int\left(\eta - \eta_d\right)dt \end{bmatrix} \quad (38)$$

From the nonlinear rotational dynamics, the torque acting on the system can be derived from the control law according to Eq. (39) .

$$\tilde{\tau}_\eta = J\left(\eta\right)\ddot{\eta} + C_m\left(\eta,\dot{\eta}\right)\dot{\eta} - T_{1\eta}^{-1}\left(J\left(\eta\right)T_\eta\dot{e}_\eta + C_m\left(\eta,\dot{\eta}\right)T_\eta e_\eta\right) + T_{1\eta}u \quad (39)$$

Therefore, this control law can be divided in three parts:

- First part is directly used for compensating the nonlinear dynamics,
- Second part is the regulator to decrease the error vector e_η and track the desired value when no disturbance influences the system,
- Third part consisting the term u is considered as an extra

1 Proportional-Integral-Derivative

control effort to compensate the disturbances affecting the system.

The matrix T_η appeared in the above equation can be written as $T_\eta = [T_{1\eta} \quad T_{2\eta} \quad T_{3\eta}]$. If this proposed control scheme is used to track the desired attitude, the dynamic equation describing the rotational motion will be summarized as follows.

$$J(\eta)T_\eta e_\eta + C_m(\eta,\eta)T_\eta e_\eta = u + d_\eta \tag{40}$$

where, $d_\eta = J(\eta)T_{1\eta}J^{-1}(\eta)d_\tau$. In fact this equation represents the error dynamics and based on this equation the nonlinear H_∞ controller design can be introduced as follows:

"Determining the control law $u(t)$ which can reduce the l_2 gain from the cost function ζ_η to the disturbance signal energy less than a defined value γ. The cost function ζ_η is introduced as equation":

$$\zeta_\eta = \begin{bmatrix} e_\eta^T & u^T \end{bmatrix} W_\eta{}^T W_\eta \begin{bmatrix} e_\eta \\ u \end{bmatrix} \tag{41}$$

and the term $W_\eta{}^T W_\eta$ which is a symmetric and positive definite matrix, can be written as Eq. (42).

$$W_\eta{}^T W_\eta = \begin{bmatrix} Q_\eta & S_\eta \\ S_\eta^T & R_\eta \end{bmatrix}, Q_\eta - S_\eta R_\eta^{-1} S_\eta \geq 0, R > 0 \tag{42}$$

If the error dynamics is rearranged in the following form:

$$\dot{e}_\eta = f_\eta(e_\eta,t) + g_\eta(e_\eta,t)u + k_\eta(e_\eta,t)d_\eta \tag{43}$$

then, a norm solution can be found satisfying Eq. (44).

$$\begin{aligned} &\frac{\partial V_\eta}{\partial t} + \frac{\partial^T V_\eta}{\partial e_\eta} f_\eta(e_\eta,t) \\ &-\frac{\partial^T V_\eta}{\partial e_\eta} g_\eta(e_\eta,t) R_\eta^{-1} S_\eta^T e_\eta + \frac{1}{2} e_\eta^T \left(Q_\eta - S_\eta R_\eta^{-1}\right. \\ &+\frac{1}{2}\left(\frac{\partial^T V_\eta}{\partial e_\eta}\right)\left(\frac{1}{\gamma^2} k_\eta(e_\eta,t) k_\eta^T(e_\eta,t)\right. \\ &\left.-g_\eta(e_\eta,t) R_\eta^{-1} g_\eta^T(e_\eta,t)\right)\left(\frac{\partial V_\eta}{\partial e_\eta}\right) = 0 \end{aligned} \tag{44}$$

For every $\gamma > \sqrt{\sigma_{max}(R_\eta)} \geq 0$, where σ_{max} indicates the maximum singular value, the optimal control law can be expressed as Eq. (45).

$$u^* = -R_\eta^{-1}\left(S_\eta^T e_\eta + g_\eta^T(e_\eta,t)\frac{\partial V_\eta(e_\eta,t)}{\partial e_\eta}\right) \tag{45}$$

Theorem 2:

Suppose a Lyapunov function $V_\eta(e_\eta,t) = \frac{1}{2} e_\eta^T T_{0\eta}^T \nu_\eta(e_\eta) T_{0\eta} e_\eta$ where, $\nu(e_\eta)$ is a symmetric and positive definite matrix with the following structure:

$$\nu_\eta(e_\eta) = \begin{bmatrix} J(\eta) & 0 & 0 \\ 0 & Y_\eta & X_\eta - Y_\eta \\ 0 & X_\eta - Y_\eta & Z_\eta + Y_\eta \end{bmatrix} \tag{46}$$

where, $X_\eta, Y_\eta, Z_\eta \in \mathbb{R}^{3\times3}$ are three symmetric and positive definite matrices and $Z_\eta - X_\eta Y_\eta^{-1} X_\eta + 2X_\eta \geq 0$. This Lyapunov function constitutes the HJB equation in Eq. (44) if the expression Eq. (47) holds.

$$\begin{aligned} &-2T_\eta^T K_\eta T_\eta + \begin{bmatrix} 0 & Y_\eta & X_\eta \\ Y_\eta & 2X_\eta & Z_\eta + 2X_\eta \\ X_\eta & Z_\eta + 2X_\eta & 0 \end{bmatrix} + Q_\eta \\ &+\frac{1}{\gamma^2} T_\eta^T T_\eta - (S_\eta^T + T_\eta)^T R_\eta^{-1}(S_\eta^T + T_\eta) = 0 \end{aligned} \tag{47}$$

Proof:

The proof of this theorem can be found in reference [19].

According to reference [24] and making simplifying assumptions similar to previous section, the control law for the rotational subsystem can be described by Eqs. (48) to (53).

$$u^* = -R_\eta^{-1}(S_\eta^T + T_\eta)e_\eta \tag{48}$$

Putting these elements into the original structure of the control law presented in Eq. (39), the overall control statement can be written as Eq. (49).

$$\tilde{\tau}_\eta^* = J(\eta_d)\ddot{\eta}_d + C_m(\eta_d,\dot{\eta}_d)\dot{\eta} - J(\eta_d)\begin{bmatrix} K_{D\eta} & K_{P\eta} & K_{I\eta}\end{bmatrix} e_\eta \tag{49}$$

For convenience, the structure of the matrices Q_η, R_η and S_η were chosen as follows.

$$Q_\eta = \begin{bmatrix} \omega_{1\eta}^2 I & 0 & 0 \\ 0 & \omega_{2\eta}^2 I & 0 \\ 0 & 0 & \omega_{3\eta}^2 I \end{bmatrix}, \quad R_\eta = r_\eta^2 I, S_\eta = \begin{bmatrix} 0 \\ 0 \\ 0 \end{bmatrix}. \tag{50}$$

As a result, the gain matrices can be calculated from the Eqs. (51) to (53).

$$K_{P\eta} = \frac{\omega_{2\eta}}{\omega_{1\eta}} I + \frac{\sqrt{\omega_{2\eta}^2 + 2\omega_{1\eta}\omega_{2\eta}}}{\omega_{1\eta}} I + J^{-1}\left(C_m + \frac{1}{r_\eta^2} I\right) \tag{51}$$

$$K_{D\eta} = \frac{\sqrt{\omega_{2\eta}^2 + 2\omega_{1\eta}\omega_{2\eta}}}{\omega_{1\eta}} I + J^{-1}\left(C_m + \frac{1}{r_\eta^2} I\right) \tag{52}$$

$$K_{I\eta} = \frac{\omega_{2\eta}}{\omega_{1\eta}} J^{-1}\left(C_m + \frac{1}{r_\eta^2} I\right) \tag{53}$$

Although a threshold γ was defined in the control design and appeared in the first expressions of the control law, it can be seen that the final expression for the gain matrices is independent from this parameter and therefore it can be used as a general expression for compensating the disturbance effects.

5- Stability Analysis

In the previous sections, two control algorithms were developed for position tracking and attitude stabilization based on Eqs. (1) and (2). In dynamic modeling, it was mentioned that the position tracking subsystem uses three independent force components to regulate the tracking error signal. Although there exists an explicit relation between three force components and euler angles based on Eq. (6), but the attitude tracking stability can not guarantee the stability of the overall cascade system solely. In fact, the error dynamic models for inner and outer loops have a coupling term which affects the stability of the cascade system. To analyze the stability behavior Eq. (54) is used which considers the coupling terms between two subsystems.

$$\begin{cases} \dot{e}_\xi = f_\xi(e_\xi) + g_\xi(e_\xi)q + k_\xi(e_\xi)w + \Delta_f(e_\eta) \\ \dot{e}_\eta = f_\eta(e_\eta) + g_\eta(e_\eta)u + k_\eta(e_\eta)d \end{cases} \tag{54}$$

where, $f_\xi, f_\eta, g_\xi, g_\eta, k_\xi$ and k_η have the same definitions as stated in Sections 3 and 4. Δ_f is the coupling term between inner and outer loop and is equal to

$$\Delta_f = T_{0\xi}^{-1}\begin{bmatrix} \frac{1}{m} \\ 0 \\ 0 \end{bmatrix} T_{1\xi} f_\Delta \tag{55}$$

where, $f_\Delta = R_t(\eta)F(t) - f_c$ and can be obtained from Eq. (56).

$$f_\Delta = u_t\begin{bmatrix} (C\phi S\theta C\psi + S\phi S\psi) - (C\phi_d S\theta_d C\psi_d + S\phi_d S\psi_d) \\ (C\phi S\theta S\psi - S\phi C\psi) - (C\phi_d S\theta_d S\psi_d - S\phi_d C\psi_d) \\ (C\phi C\theta) - (C\phi_d C\theta_d) \end{bmatrix} \tag{56}$$

Following lemmas are introduced to analyze the stability of cascade NL H_∞ system for Eq. (54) based on [28, 30-31].

Lemma 1

If there exists a proper solution $V \geq 0$ for HJB equation and the system $\dot{x} = f(x)$ in Eq. (57) is zero state observable, Then $V(x) > 0$ for $x \neq x_0$, and the closed-loop system defined by Eq. (57) is Globally Asymptotically Stable (GAS).

$$\begin{aligned} &x = f(x) + g(x)u + k(x)d, \\ &y = h(x), f(x_0) = 0, h(x_0) = 0 \\ &u = -g^T \frac{\partial^T V}{\partial x}(x) \end{aligned} \tag{57}$$

Lemma 2

The system $\dot{e}_\xi = \tilde{f}\left(e_\xi, e_\eta, d\right)$ is Input-to-State Stable (ISS) if and only if there exists a $\mathcal{C}^1$ positive definite radially unbounded function $V\left(e_\xi\right)$ such that:

$$\| e_\xi \| \geq \mathcal{X}_1\left(\| e_\xi \|\right) \Rightarrow \frac{\partial^T V\left(e_\xi\right)}{\partial e_\xi} \tilde{f}\left(e_\xi, e_\eta, d\right) \leq -\mathcal{X}_2\left(\| e_\xi \|\right) \quad (58)$$

where, $\mathcal{X}_1$ and $\mathcal{X}_2$ are two class $\mathcal{K}$ functions.

Lemma 3

If the system $\dot{e}_\xi = \tilde{f}\left(e_\xi, e_\eta, d\right)$ is ISS, then if $e_\xi = 0$ is a GAS equilibrium point for $\dot{e}_\xi = f_1\left(e_\xi\right)$, and there exists a $\mathcal{C}^1$ partial state feedback control $u = k\left(e_\eta\right)$ such that the equilibrium point $e_\eta = 0$ of $\dot{e}_\eta = f_2\left(e_\eta\right)$ is GAS, then the feedback $u = k\left(e_\eta\right)$ achieves GAS of the equilibrium $\left(e_\xi, e_\eta\right) = (0,0)$ of the cascade Eq. (54)

Using the above lemmas, the problem is reduced to prove the following theorem to ensure that the cascade system controlled by q^* and u^* guarantees the stability of the system.

Theorem 3:

Given the system in Eq. (54), the control laws q^* from Eq. (32) and u^* from Eq. (48) guarantee the asymptotic stability of the equilibrium point $\left(e_\xi, e_\eta\right) = (0,0)$, if all conditions presented in lemma 2 hold.

Proof:

According to Eqs. (54) to (56) for the coupling term, the following relation can be written:

$$\| \Delta_f \| = \frac{1}{m} |u_t| \| H\left(\delta\eta, e_\xi\right) \| \quad (59)$$

where, $\delta\eta = \eta - \eta_d$ and $H\left(\delta\eta, e_\xi\right)$ is defined in Eq. (66).

$$H\left(e_\xi, \delta\eta\right) = \begin{bmatrix} h_1(t) & h_2(t) & h_3(t) & 0 & 0 & 0 & 0 & 0 & 0 \end{bmatrix}$$

$$\begin{aligned} h_1(t) &= \left(C\phi S\theta C\psi + S\phi S\psi\right) \\ &\quad -\left(C\phi_d S\theta_d C\psi_d + S\phi_d S\psi_d\right) \\ h_2(t) &= \left(C\phi S\theta S\psi - S\phi C\psi\right) \\ &\quad -\left(C\phi_d S\theta_d S\psi_d - S\phi_d C\psi_d\right) \\ h_3(t) &= C\phi C\theta - C\phi_d C\theta_d \end{aligned} \quad (60)$$

On the other hand, $|u_t|$ can be obtained from Eq. (61) as follows:

$$|u_t| = \| f_c^* \| = m \| \ddot{\xi}_d + \frac{1}{m} K_\xi \dot{\xi} + G - \begin{bmatrix} K_{D\xi} & K_I \end{bmatrix} \quad (61)$$

According to NL H_∞ problem definition, if $w \in \mathcal{L}_2(0,\infty)$, then for any limited initial state vector, the values of f_c^* and e_ξ remain in $\mathcal{L}_2(0,\infty)$ and relations through Eq. (62) are satisfied.

$$\begin{aligned} &\| \ddot{\xi}_d + \frac{1}{m} K_\xi \dot{\xi} \| \leq \| \ddot{\xi}_d \| + \| \frac{1}{m} K_\xi \dot{\xi} \| \leq l_\xi, \\ &|u_t| \leq m\left(\| \ddot{\xi}_d + \frac{1}{m} \dot{\xi} \| + g + \| \begin{bmatrix} K_{D\xi} & K_{P\xi} & K_{I\xi} \end{bmatrix} e_\xi \| \right) \\ &\leq m\left(l_\xi + g\right) + \| \begin{bmatrix} K_{D\xi} & K_{P\xi} & K_{I\xi} \end{bmatrix} e_\xi \| \end{aligned} \quad (62)$$

where, $l_\xi = \| \ddot{\xi}_d \|_\infty + \| \frac{1}{m} K_\xi \dot{\xi} \|_\infty$. If $l_c = \max\left\{ \| K_{D\xi} \|, \| K_{P\xi} \|, \| K_{I\xi} \| \right\}$, then Eq. (63) is obtained.

$$\| \begin{bmatrix} K_{D\xi} & K_{P\xi} & K_{I\xi} \end{bmatrix} e_\xi \| \leq l_c \| e_\xi \| \quad (63)$$

Hence, $|u_t|$ establishes the following inequalities.

$$|u_t| \leq \begin{cases} 2l_c \| e_\xi \| \; if \; \| e_\xi \| \geq \dfrac{m}{l_c\left(g + l_\xi\right)} \\ 2m\left(g + l_\xi\right) if \; \| e_\xi \| \leq \dfrac{m}{l_c\left(g + l_\xi\right)} \end{cases} \quad (64)$$

In addition, based on reference [28], the following relations are satisfied for $h_1(t), h_2(t)$ and $h_3(t)$.

$$\begin{cases} h_1^2 \leq \zeta_1\left(\delta\phi^2 + \delta\theta^2 + \delta\psi^2\right) \\ h_2^2 \leq \zeta_2\left(\delta\phi^2 + \delta\theta^2 + \delta\psi^2\right) \\ h_3^2 \leq \zeta_3\left(\delta\phi^2 + \delta\theta^2\right) \end{cases} \quad (65)$$

where, ζ_1, ζ_2 and ζ_3 are three positive constants. Accordingly $\| H\left(e_\xi, \delta\eta\right) \|$ is satisfied in Eq. (66).

$$\| H\left(e_\xi, \delta\eta\right)\| = \sqrt{h_1^2+h_2^2+h_3^2} \le \sqrt{\sum_{i=1}^{3}\zeta_i}\ \|\delta\eta\| \quad (66)$$

Now, assuming $C_1 = \frac{m\left(g+l_\xi\right)}{l_c} > 0$, the following inequality is also satisfied.

$$\|e_\xi\| \ge C_1 \Rightarrow \|\Delta_f\| \le \frac{2l_c}{m}\sqrt{\sum_{i=1}^{3}\zeta_i}\ \|\delta\eta\|\|e_\xi\| \quad (67)$$

Defining $V_1\left(e_\eta\right) = \frac{1}{2}e_\eta^T e_\eta$, and differentiating it with respect to time, and using the error dynamics, we have

$$\begin{aligned}\frac{\partial^T V_1}{\partial e_\xi}\tilde{f}\left(e_\xi, e_\eta\right) = \\ -e_\xi^T\left(-R_1 + R_2\begin{bmatrix}K_{D\xi} & K_{P\xi} & K_{I\xi}\end{bmatrix}\right)e_\xi \\ +\frac{1}{m}e_\xi^T R_2 d_\xi + e_\xi^T\Delta_f\end{aligned} \quad (68)$$

where, $R_1 = \begin{bmatrix}0 & 0 & 0\\ I & 0 & 0\\ 0 & I & 0\end{bmatrix}$ and $R_2 = \begin{bmatrix}I\\0\\0\end{bmatrix}$. Accordingly, it can be written that:

$$\begin{aligned}\frac{\partial^T V_1}{\partial e_\xi}\tilde{f}\left(e_\xi, e_\eta\right) \le -\| e_\xi\|\|-R_1 e_\xi \\ +R_2\begin{bmatrix}K_{D\xi} & K_{P\xi} & K_{I\xi}\end{bmatrix}e_\xi\| \\ +\frac{1}{m}\|d_\xi\|\|e_\xi\| + \kappa\left(\|\delta\eta\|\right) \quad \|e_\xi\|^2 \text{ for } \|e_\xi\| \ge C_1\end{aligned} \quad (69)$$

Hence,

$$\begin{aligned}&\frac{\partial^T V_1}{\partial e_\xi}\tilde{f}\left(e_\xi, e_\eta\right) \le -\|e_\xi\| \\ &\times\left(\|e_\xi + l_c\|e_\xi\| - \frac{1}{mC_1}\|d_\xi\|_\infty\|e_\xi\| - \kappa\left(\|\delta\eta\|\right)\|e_\xi\|\right) \\ &\left(\|e_\xi + l_c\|e_\xi\| - \frac{1}{mC_1}\|d_\xi\|_\infty\|e_\xi\| - \kappa\left(\|\delta\eta\|\right)\|e_\xi\|\right) \\ &\le -\left(\left(1+l_c\right) - \frac{1}{mC_1}\|d_\xi\|_\infty - \kappa\left(\|\delta\eta\|\ \right)\right)\|e_\xi\|^2\end{aligned} \quad (70)$$

Since, $\|\delta\eta\|_\infty$ and $\|d_\xi\|_\infty$ are both bounded, if l_c is chosen large enough, then

$$\mathcal{X}_2\left(e_\xi\right) = \left(1 + l_c - \frac{1}{mC_1}\|d_\xi\|_\infty - \kappa\left(\|\delta\eta\|_\infty\right)\right)\|e_\xi\|^2 \quad (71)$$

is a class $\mathcal{K}$ function. On the other hand, $\mathcal{X}_1\left(\|e_\xi\|\right) = \sqrt{C_1\|e_\xi\|}$ is a class $\mathcal{K}$ function which satisfies the inequality $C_1 \le \mathcal{X}_1\left(\|e_\xi\|\right) \le \|e_\xi\|$. Using $\mathcal{X}_1\left(\|e_\xi\|\right)$ and $\mathcal{X}_2\left(\|e_\xi\|\right)$ Eq. (72) yields:

$$\|e_\xi\| \ge \mathcal{X}_1\left(e_x i\right) \Rightarrow \frac{\partial^T V_1}{\partial e_\xi}\tilde{f}\left(e_\xi, e_\eta\right) \le -\mathcal{X}_2\left(e_\xi\right) \quad (72)$$

which means $\dot{e}_\xi = \tilde{f}\left(e_\xi, e_\eta\right)$ is ISS according to lemma 2.

On the other hand, based on lemma 1 and using $V_\xi\left(e_\xi\right)$ and $V_\eta\left(e_\eta\right)$ defined in Sections 3 and 4, it can be concluded that $\dot{e}_\xi = f_\xi + g_\xi q^* + k_\xi w$ and $\dot{e}_\eta = f_\eta + g_\eta u^* + k_\eta d$ are both GAS at $e_\xi = 0$ and $e_\eta = 0$. Therefore, all conditions stated through lemma 1, 2 and 3 are established and Theorem 3 is proved. Accordingly, the asymptotic stability of the equilibrium point $\left(e_\xi, e_\eta\right) = (0,0)$ for the cascade system is guaranteed by using q^* and u^* obtained in Eqs. (36) and (54) as control laws for outer and inner loops.

6- Simulation Results

In this section, simulation results are presented to show the effectiveness of the algorithm discussed in the previous sections. To implement the algorithm, data presented in Table 1 are utilized. Nominal values for dynamic simulation parameters are taken from reference [29].

To implement the control algorithm a block diagram is used as shown in Fig. 1.

The defined mission for the simulation consists of three parts:

A curved path in the horizontal plane and a smooth climb phase.

A translataion along a semi rectangular path in the horizontal plane and maintaining the altitude,

Vertical descent to the base altitude without any translation in horizontal plane.

On the other hand, random forces and moments acting on the system were assumed as environmental zero-mean disturbances. Another type of perturbation acting on the system, is a sustained disturbance modeled as a step function with random acting moment and applied on each force and moment components, independently. The measurement vectors included a noise assumed to be zero-mean and Gaussian.

Monte-Carlo simulations were accomplished by repeating the above scenario 1000 times and evaluating the mean behavior and the standard deviations for flight parameters and performance indexes. To show a more explicit view of the system performance, two numerical indexes were introduced. The Integral Square Error (ISE) and the Integral of the Absolute value of the control Derivative (IADU) [29] indexes were obtained for states and control signals, respectively.

Fig. 2, shows the position tracking error and its variation

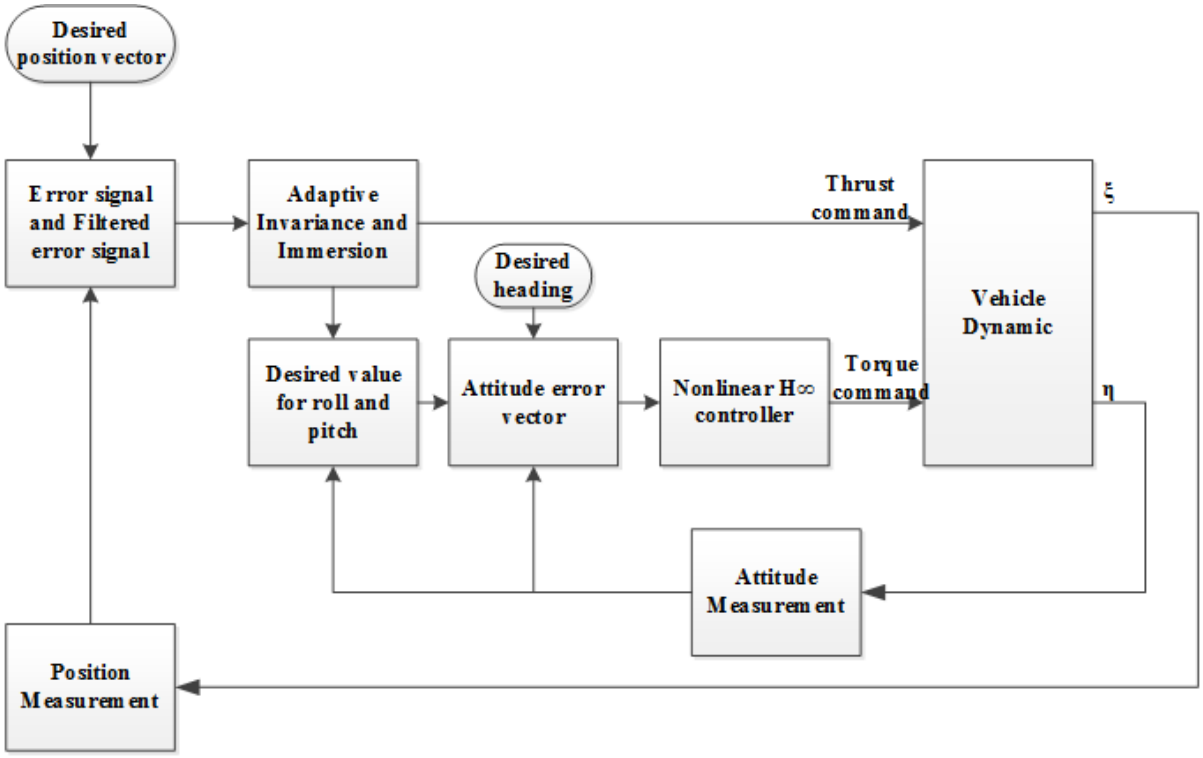

Fig. 1. Block diagram used for simulation

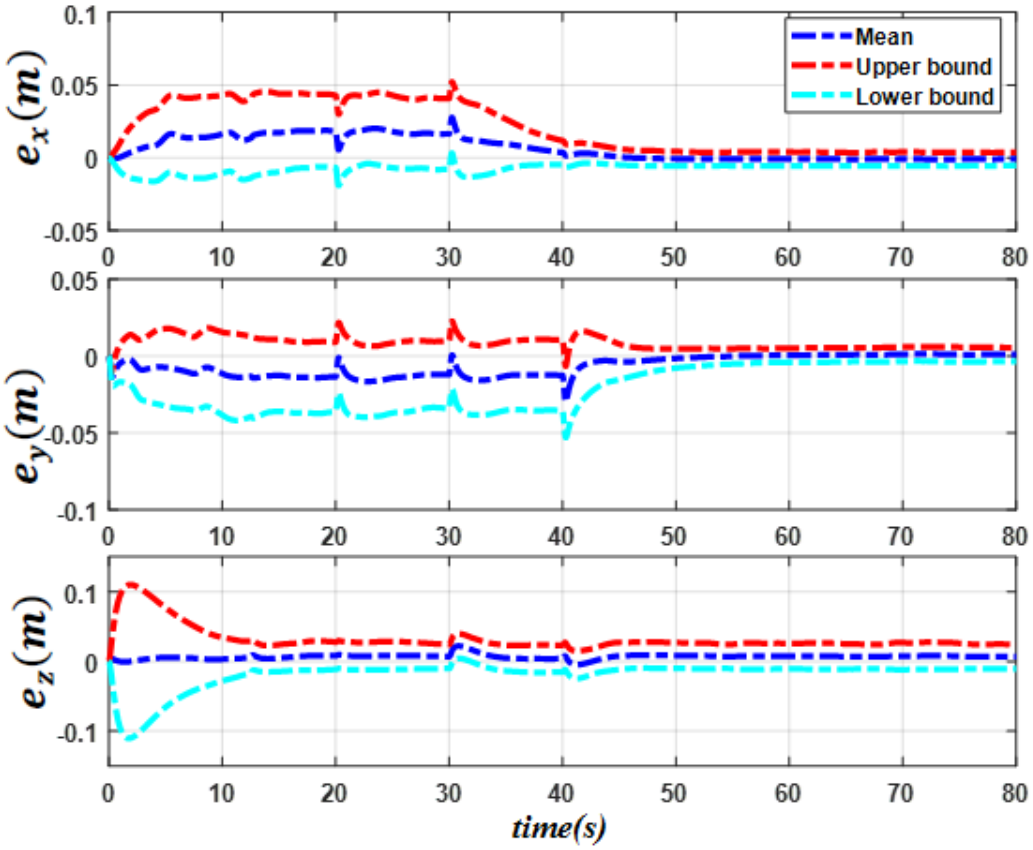

Fig. 2. Position tracking for defined mission

Table 1. Simulation and controller data

Parameter	Value
General Parameters	
Weight	7.26 N
Weight uncertainty	50%
I_{xx}	4e-3 kg.m ^{2}
I_{yy}	4e-3 kg.m ^{2}
I_{zz}	8e-3 kg.m ^{2}
I_{xy}	4e-4 kg.m ^{2}
Inertia uncertainty	50%
ξ_0 (m)	$[0 \quad 0.5 \quad 0.5]$
η_0 (deg)	[0 0 0.5]
K_ξ	$[0.01 \quad 0.01 \quad 0.01]$
K_ξ uncertainty	50%
K_η	$[0.01 \quad 0.01 \quad 0.01]$
K_η uncertainty	50%
Inner-loop controller parameters	
r_η	1.5
$\omega_{1\eta}$	0.1
$\omega_{2\eta}$	5
$\omega_{3\eta}$	15
Outer-loop controller parameters	
r_ξ	1
$\omega_{1\xi}$	1.2
$\omega_{2\xi}$	5
$\omega_{3\xi}$	2

bounds. It can be seen that the state error vector converges to zero asymptotically. Accordingly, the system has an excellent robustness against uncertainty and external deterministic disturbances.

Fig. 3, shows the three-dimensional view of the simulation results for the defined mission. As shown, the difference between mean conditions for the position vector and its estimation was found to be insignificant.

The performance of the attitude stabilization and robustness against parameter uncertainty and external disturbances is depicted in Fig. 4. It can be seen that the cascade system has an appropriate tracking performance in the presence of model uncertainty and disturbance attenuation. Utilizing integral actions in both inner and outer loops causes the full elimination of the force and moment disturbances arisen from unexpected conditions, as shown in Figs. 3 and 4.

Statistical results of ISE index for position tracking errors are depicted as a box-plot presented in Fig. 5. According to this figure, the tracking performance in horizontal plane was obtained to be more accurate, and the altitude control more sensitive to disturbances acting on the system.

The ISE index for the error signals in Euler angles is depicted in Fig. 6. Based on these results, the proposed algorithm shows an acceptable performance in stabilizing the attitude dynamics in a general mission.

Moreover, for statistical analysis on control efforts in this mission, the IADU index is shown for the net force and three components of torque vector in Fig. 7.

As mentioned earlier, for a quantitative comparison, ISE index was obtained for state tracking performance. Table 2 demonstrates the comparison of ISE index for the suggested cascade system and two previous algorithms based on MPC plus NL H_∞, and Backstepping methods. As depicted in this Table, ISE index has decreased for all states, which means an acceptable tracking performance in similar conditions compared to other algorithms.

The values of IADU index are also compared in Table 3 for cascade NL H_∞ implementation and two previous methods simulated in reference [19]. As listed in this Table, the values attained for this index were found to be less than other algorithms.

Considering the discussed results and quantitative comparisons made based on ISE and IADU indexes, it can be concluded that the proposed scheme for controller design has an acceptable robust performance in the presence of parameter uncertainties, exogenous disturbances and measurements noise. Moreover, the stability of the system examined by simulations is consistent with the analytical stability establishment in Section 5.

7- Conclusions

In this paper, a cascade NL H_∞ scheme was suggested for position tracking problem consisting inner-loop and outer-loop controllers to stabilize the rotational motion and track the desired flight path, respectively. To achieve a reliable and appropriate performance in position tracking, a NL H_∞ control algorithm was developed for compensating the parametric uncertainties especially in inertial parameters and rejecting exogenous disturbances. For the inner-loop controller, another nonlinear H_∞ algorithm was implemented based on reference [19] together with an integral action to decrease the steady state errors in presence of sustained disturbances and improve the tracking results. The proof of stability was accomplished using existing theorem for cascade systems and examined numerically by Monte-Carlo simulations. For this reason, 1000 simulations were performed and for each of them a set of model parameters was sampled due to variation bounds assuming a uniform distribution. In addition, other stochastic parts of the simulation such as measurements noise, atmospheric random disturbances and random action time for sustained disturbances were changed in each simulation. Simulation results for flight parameters were depicted by the mean behavior and the upper and lower bounds with respect to standard deviation index. To show more explicit results

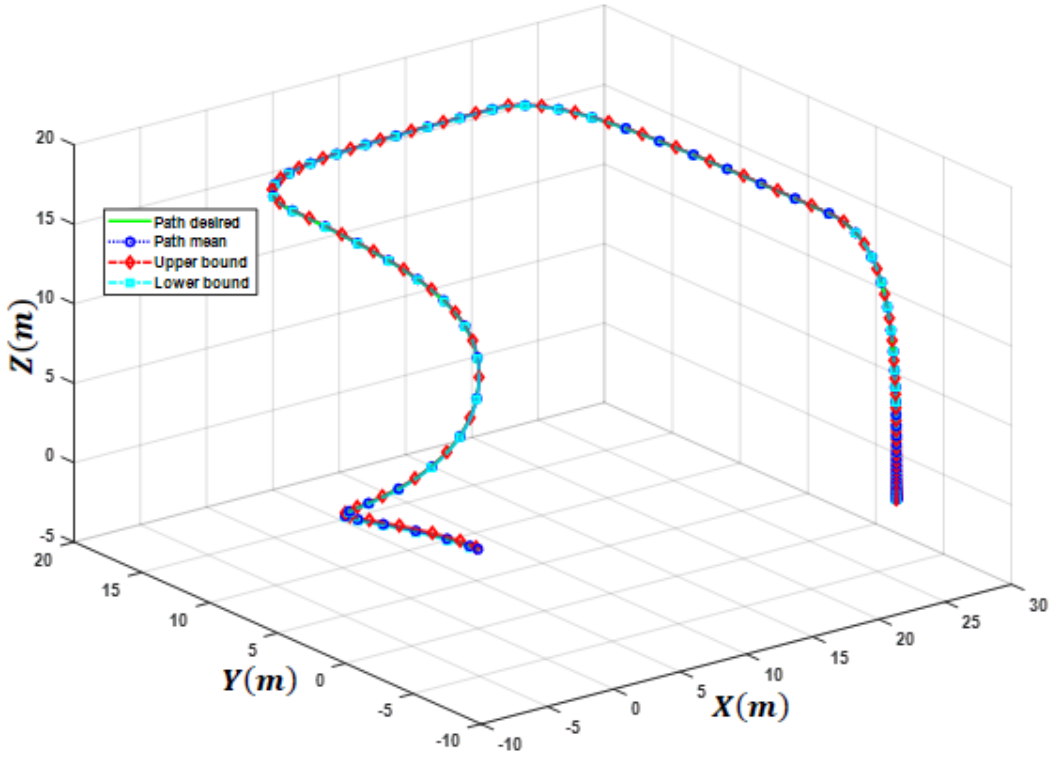

Fig. 3. 3D thrajectory for defined mission

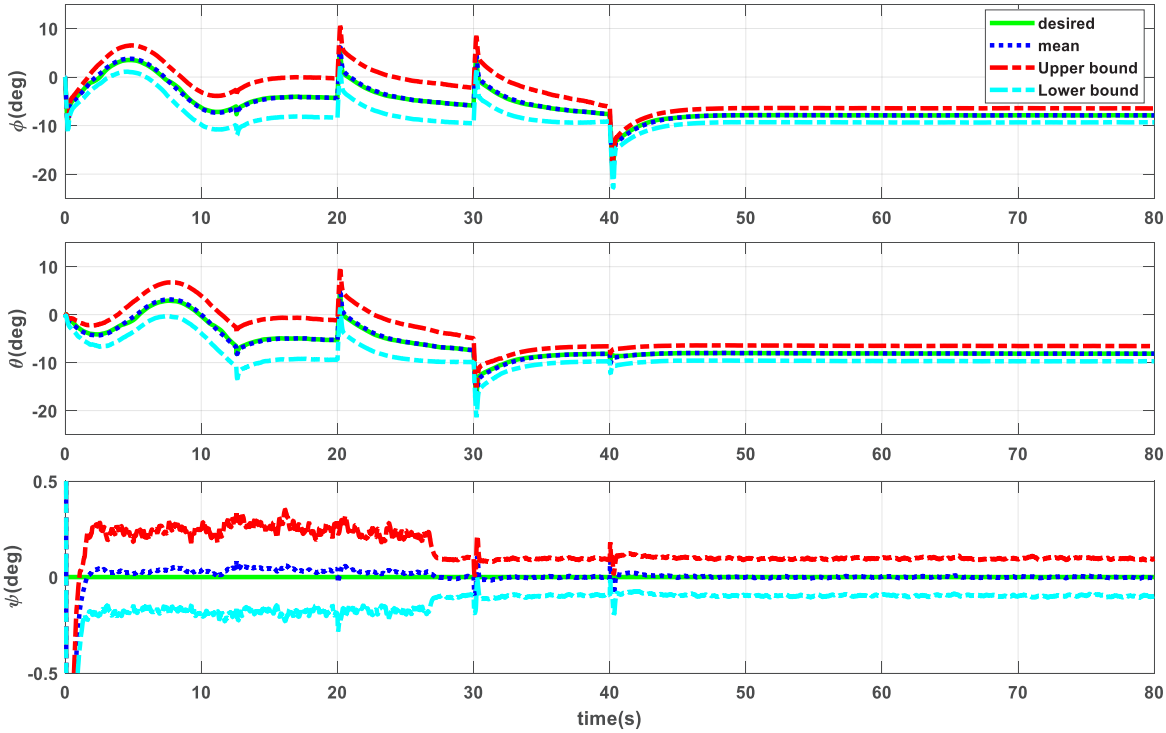

Fig. 4. Euler angles for the first scenario

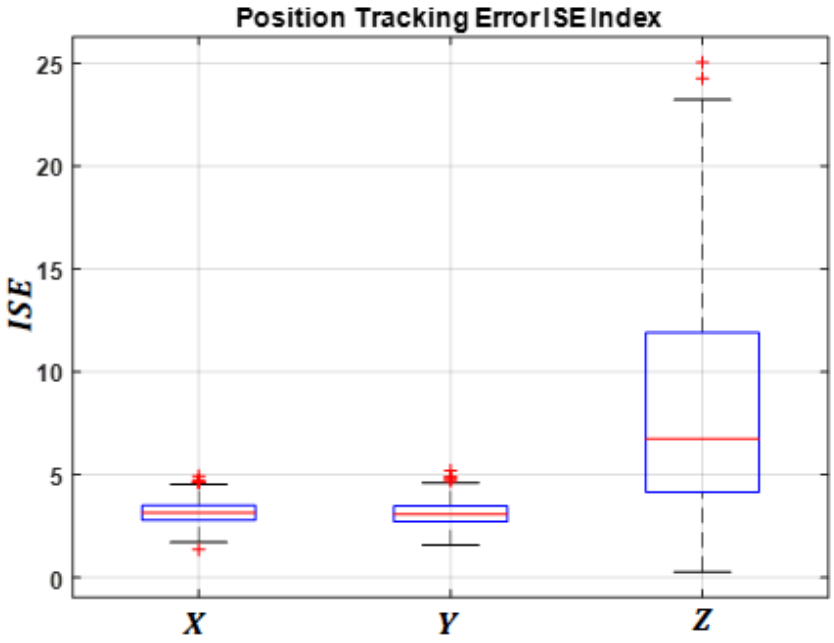

Fig. 5. Control forces acting on the system in the second path following scenario

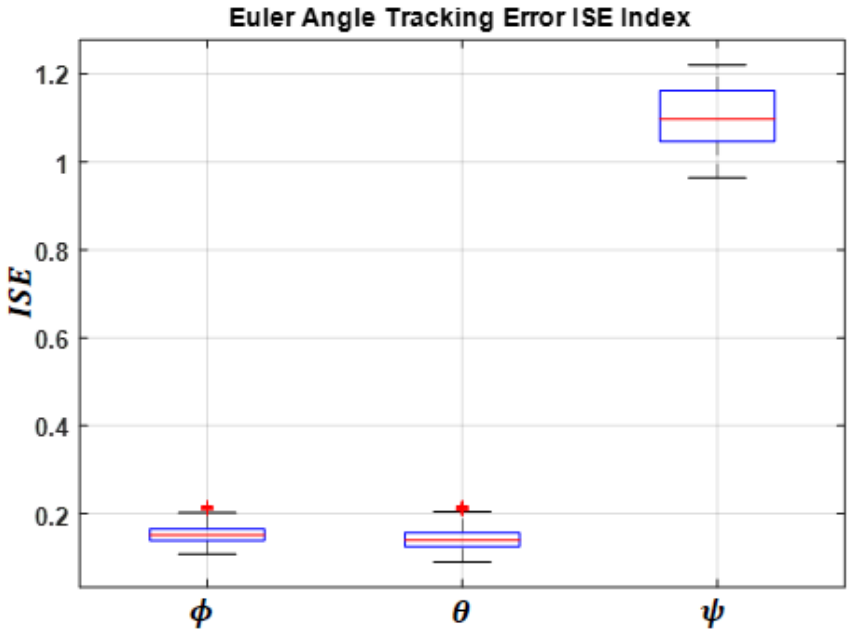

Fig. 6. Control torques acting on the system in the second path following scenario

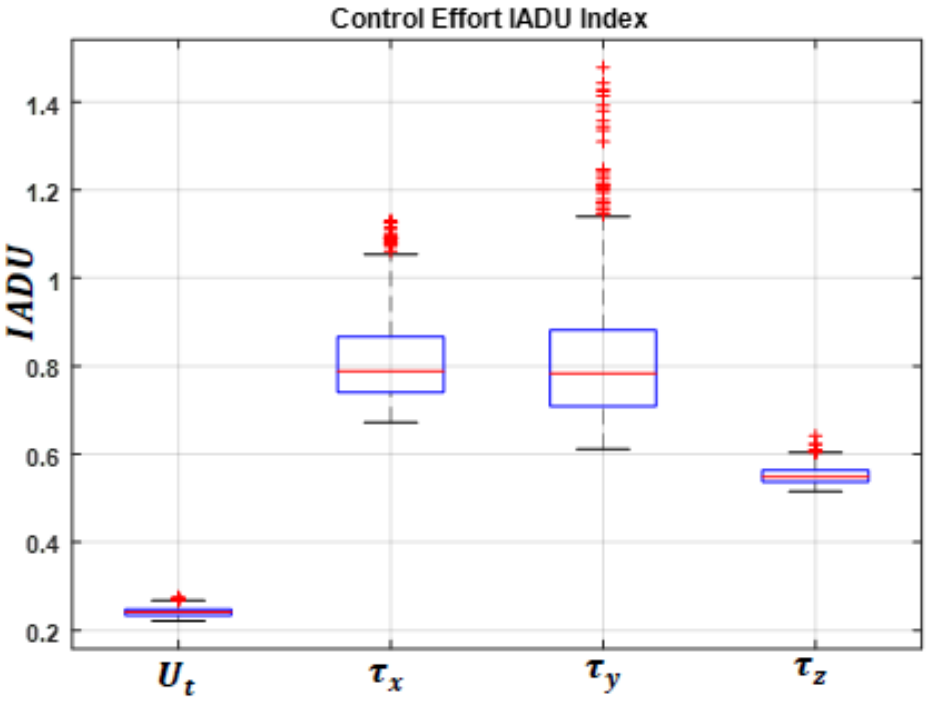

Fig. 7. Control torques acting on the system in the second path following scenario

Table 2. Mean-ISE index performance comparison

States	Cascade NL H_∞	MPC+NL H_∞	Backstepping
x	3.14	18.28	26.14
y	3.1	16.44	22.06
z	8.28	11.29	19.020
ϕ	0.15	4.63	19.43
θ	0.14	4.78	8.063
ψ	1.108	4.62	5.22

on tracking errors and control efforts, two ISE and IADU indexes were used. The box plots were used to show the mean and variation bounds for these indexes in the predefined mission. According to these results and comparing them with other methods, it can be seen that the error compensation performance was comparable with algorithms presented by reference [19, 28]. Further investigations should involve the practical implementation on a real quadrotor. Because of the convenient architecture of the proposed controller and straightforward calculations in control laws for both inner and outer loops, all standard robotic control boards like Raspberry Pi can be nominated for hardware implementation.

Table 3. Mean-IADU index performance comparison

Control Signal	Cascade NL H_∞	MPC+NL H_∞	Backstepping
U_t	2.42	17.6692	20.8502
τ_x	8.14	63.955	199.97
τ_y	8.13	65.417	220.38
τ_z	5.51	18.714	43.1515

References

[1] P. Castillo, R. Lozano, A. Dzul, Stabilization of a mini-rotorcraft having four rotors, in: 2004 IEEE/RSJ International Conference on Intelligent Robots and Systems (IROS)(IEEE Cat. No. 04CH37566), IEEE, 2004, pp. 2693-2698.

[2] S. Roelofsen, D. Gillet, A. Martinoli, Reciprocal collision avoidance for quadrotors using on-board visual detection, in: 2015 IEEE/RSJ International Conference on Intelligent Robots and Systems (IROS), IEEE, 2015, pp. 4810-4817.

[3] A. Shukla, H. Karki, Application of robotics in onshore oil and gas industry—A review Part I, Robotics and Autonomous Systems, 75 (2016) 490-507.

[4] J.J. Lugo, A. Zell, Framework for autonomous on-board navigation with the AR. Drone, Journal of Intelligent & Robotic Systems, 73(1-4) (2014) 401-412.

[5] W. Dong, G.-Y. Gu, X. Zhu, H. Ding, Development of a quadrotor test bed—modelling, parameter identification, controller design and trajectory generation, International Journal of Advanced Robotic Systems, 12(2) (2015) 7.

[6] F. Kendoul, Z. Yu, K. Nonami, Guidance and nonlinear control system for autonomous flight of minirotorcraft unmanned aerial vehicles, Journal of Field Robotics, 27(3) (2010) 311-334.

[7] N. Cao, A.F. Lynch, Inner–outer loop control for quadrotor UAVs with input and state constraints, IEEE Transactions on Control Systems Technology, 24(5) (2016) 1797-1804.

[8] M. Hayajneh, M. Melega, L. Marconi, Design of autonomous smartphone based quadrotor and implementation of navigation and guidance systems, Mechatronics, 49 (2018) 119-133.

[9] J. Guerrero-Castellanos, N. Marchand, A. Hably, S. Lesecq, J. Delamare, Bounded attitude control of rigid bodies: Real-time experimentation to a quadrotor mini-helicopter, Control Engineering Practice, 19(8) (2011) 790-797.

[10] J. Kim, M.-S. Kang, S. Park, Accurate modeling and robust hovering control for a quad-rotor VTOL aircraft, in: Selected papers from the 2nd International Symposium on UAVs, Reno, Nevada, USA June 8–10, 2009, Springer, 2009, pp. 9-26.

[11] H. Liu, Y. Bai, G. Lu, Y. Zhong, Robust attitude control of uncertain quadrotors, IET Control Theory & Applications, 7(11) (2013) 1583-1589.

[12] Y. Wang, Y. Chenxie, J. Tan, C. Wang, Y. Wang, Y. Zhang, Fuzzy radial basis function neural network PID control system for a quadrotor UAV based on particle swarm optimization, in: 2015 IEEE International Conference on Information and Automation, IEEE, 2015, pp. 2580-2585.

[13] C. Peng, Y. Bai, X. Gong, Q. Gao, C. Zhao, Y. Tian, Modeling and robust backstepping sliding mode control with Adaptive RBFNN for a novel coaxial eight-rotor UAV, IEEE/CAA Journal of Automatica Sinica, 2(1) (2015) 56-64.

[14] C. Nicol, C. Macnab, A. Ramirez-Serrano, Robust adaptive control of a quadrotor helicopter, Mechatronics, 21(6) (2011) 927-938.

[15] A.C. Satici, H. Poonawala, M.W. Spong, Robust optimal control of quadrotor UAVs, IEEE Access, 1 (2013) 79-93.

[16] C. Mu, Y. Zhang, Learning-Based Robust Tracking Control of Quadrotor With Time-Varying and Coupling Uncertainties, IEEE transactions on neural networks and learning systems, (2019).

[17] N. Koksal, M. Jalalmaab, B. Fidan, Adaptive Linear Quadratic Attitude Tracking Control of a Quadrotor UAV Based on IMU Sensor Data Fusion, Sensors, 19(1) (2019) 46.

[18] O. Mofid, S. Mobayen, Adaptive sliding mode control for finite-time stability of quad-rotor UAVs with parametric uncertainties, ISA transactions, 72 (2018) 1-14.

[19] F. Rekabi, F.A. Shirazi, M.J. Sadigh, ADAPTIVE-NONLINEAR H∞ HIERARCHICAL ALGORITHM FOR QUADROTOR POSITION TRACKING, in: 2018 6th RSI International Conference on Robotics and Mechatronics (IcRoM), IEEE, 2018, pp. 12-17.

[20] W. Lei, C. Li, M.Z. Chen, Robust Adaptive Tracking Control for Quadrotors by Combining PI and Self-Tuning Regulator, IEEE Transactions on Control Systems

Technology, (2018).
[21] J. Moreno-Valenzuela, R. Pérez-Alcocer, M. Guerrero-Medina, A. Dzul, Nonlinear PID-Type Controller for Quadrotor Trajectory Tracking, IEEE/ASME Transactions on Mechatronics, 23(5) (2018) 2436-2447.
[22] H. Ríos, R. Falcón, O.A. González, A. Dzul, Continuous Sliding-Mode Control Strategies for Quadrotor Robust Tracking: Real-Time Application, IEEE Transactions on Industrial Electronics, 66(2) (2019) 1264-1272.
[23] A. L'afflitto, R.B. Anderson, K. Mohammadi, An Introduction to Nonlinear Robust Control for Unmanned Quadrotor Aircraft: How to Design Control Algorithms for Quadrotors Using Sliding Mode Control and Adaptive Control Techniques [Focus on Education], IEEE Control Systems, 38(3) (2018) 102-121.
[24] G.V. Raffo, M.G. Ortega, F.R. Rubio, Path tracking of a UAV via an underactuated control strategy, European Journal of Control, 17(2) (2011) 194-213.
[25] L. Luque-Vega, B. Castillo-Toledo, A.G. Loukianov, Robust block second order sliding mode control for a quadrotor, Journal of the Franklin Institute, 349(2) (2012) 719-739.
[26] H. Liu, J. Xi, Y. Zhong, Robust hierarchical control of a laboratory helicopter, Journal of the Franklin Institute, 351(1) (2014) 259-276.
[27] H. Liu, D. Li, J. Xi, Y. Zhong, Robust attitude controller design for miniature quadrotors, International Journal of Robust and Nonlinear Control, 26(4) (2016) 681-696.
[28] B. Zhao, B. Xian, Y. Zhang, X. Zhang, Nonlinear robust sliding mode control of a quadrotor unmanned aerial vehicle based on immersion and invariance method, International Journal of Robust and Nonlinear Control, 25(18) (2015) 3714-3731.
[29] G.V. Raffo, M.G. Ortega, F.R. Rubio, An integral predictive/nonlinear H∞ control structure for a quadrotor helicopter, Automatica, 46(1) (2010) 29-39.
[30] R. Sepulchre, M. Jankovic, P.V. Kokotovic, Constructive nonlinear control, Springer Science & Business Media, 2012.
[31] A.J. Van Der Schaft, L/sub 2/-gain analysis of nonlinear systems and nonlinear state-feedback h/sub infinity/ control, IEEE transactions on automatic control, 37(6) (1992) 770-784.